Tunneling of optical lattice solitons at interfaces

Lasha Tkeshelashvili*

Andronikashvili Institute of Physics, Tamarashvili 6, 0177 Tbilisi, and Tbilisi State University, Chavchavadze 3, 0128 Tbilisi, Georgia

(Received 14 June 2012; published 25 September 2012)

The nonlinear wave propagation and scattering processes in discrete optical heterostructures is studied both analytically and numerically. The presented theory describes the reflection and tunneling of lattice solitons at interfaces. In particular, the derived expressions allow us to construct the reflected and transmitted pulses from the incident one. In the range of validity, the analytical results are in very good agreement with the numerical simulations. It is demonstrated that optical heterostructures represent an effective tool for controlling and manipulating nonlinear light pulses and beams.

DOI: 10.1103/PhysRevA.86.033836 PACS number(s): 42.65.Tg, 42.25.Gy, 42.70.Qs

I. INTRODUCTION

Nanostructured periodic systems such as photonic crystals and metamaterials provide the opportunity to realize unique optical phenomena not found in nature [1,2]. Recently, essential progress was reported in the modeling and fabrication of various dielectric and metallodielectric structures. Examples include the demonstration of the photonic band-gap effect [3–5], the slow-light regime [6–8], and enhanced light-matter interaction processes [9,10], to mention just a few. Effective control of photons in nanostructured photonic band-gap systems can be achieved by means of an engineered network of waveguide channels, nanocavities, and other functional elements. That is, any practical realization of all-optical communication networks will represent a heterostructure of different units in which light pulses can be effectively controlled and manipulated.

Solitons are nonlinear wave packets that can propagate undistorted over long distances. This particular feature makes them very attractive for applications in the field of all-optical communications [11]. However, the problem of soliton interaction processes with inhomogeneities needs to be addressed separately. The point is that solitons represent solutions of so-called integrable nonlinear equations [12]. The inhomogeneity may break the integrability of the model and, as a result, cause the radiative decay of solitons [13].

Let us consider the case of effectively one-dimensional discrete optical systems [14]. In particular, discrete wave dynamics was intensively studied in arrays of optical waveguides [15], coupled nanocavities in photonic crystals [16], metallodielectric systems [17,18], and Bose-Einstein condensates in deep optical lattices [19–21]. Under many experimentally accessible conditions the governing equation for such systems is the discrete nonlinear Schrödinger equation [22]:

$$i\frac{\partial \psi_n}{\partial t} + C(\psi_{n+1} + \psi_{n-1}) + N|\psi_n|^2\psi_n + \varepsilon_n\psi_n = 0. \quad (1)$$

Here, depending on the system under consideration, t is either the temporal or the spatial variable [14]. The eigenmode amplitude at site n is ψ_n, and C represents the coupling constant of the adjacent sites. In what follows, for the sake of simplicity, it is assumed that C has the same value for all sites. Moreover, the nonlinear coefficient N is also assumed to be independent of n. The inhomogeneity in Eq. (1) is introduced through ε_n. For instance, in the case of arrays of optical waveguides, ε_n may change from site to site due to the different refractive constant of the individual waveguides.

Below, nonlinear wave transmission and reflection are studied in discrete optical heterostructures which consist of two semi-infinite uniform elements with a step discontinuity at the interface. The demonstration of surface solitons in such systems [23–25] initiated the rapidly growing interest in linear and nonlinear optical wave dynamics at interfaces [26–29]. In particular, the power-dependent behavior of lattice solitons at the interface between two periodic media was reported in Refs. [30] and [31]. In what follows, soliton propagation and scattering are studied in the weakly nonlinear limit, i.e., when the nonlinear term in Eq. (1) represents a small perturbation to the linear part.

Before proceeding further, the following comment is in order. Localized wave packets are called pulses for systems where t represents the temporal variable. However, if t is the spatial coordinate, those pulses actually are optical beams. In particular, that is the case for arrays of coupled waveguides.

II. PERTURBATION ANALYSIS

If nonlinear effects are sufficiently weak, the problem can be treated analytically. In this limiting case, by means of the reductive perturbation method [32,33], Eq. (1) can be reduced to the integrable nonlinear Schrödinger (NLS) equation [11]. The NLS model describes the carrier wave envelope, and under certain conditions, it supports the bright soliton solutions [12]. From the physics point of view, soliton formation is a result of the balance between nonlinear effects and linear dispersion and diffraction. In order to achieve such a balance, the wave envelope must vary slowly on the scale of the carrier wavelength. For low enough pulse amplitudes this condition can always be satisfied. Indeed, envelope soliton parameters depend on the strength of nonlinear effects. In particular, a wider soliton has a lower amplitude [12]. Therefore, the theory presented is valid for the case of sufficiently wide solitons.

Let us assume that $\varepsilon_n = \varepsilon_l$ for $n < 0$ and $\varepsilon_n = \varepsilon_r$ for $n \geqslant 0$. That is, the system is uniform on both sides of the interface which is located at $n = 0$. Furthermore, suppose that an incident nonlinear pulse in the left region ($n < 0$) propagates to the right and gets scattered at the interface. In general,

*lashat@mail.com

in the final state, there will be a reflected wave propagating backwards to the left and a transmitted wave which tunnels at the interface in the right region ($n \geqslant 0$).

It should be stressed that only the variation in ε_n is relevant for wave propagation and scattering processes. Indeed, the values of ε_n in the corresponding term in Eq. (1) can be shifted by the arbitrary constant ε via $\psi_n \to \exp(i\varepsilon t)\psi_n$ transformation. Therefore, without loss of generality, either ε_l or ε_r can be made to equal exactly 0.

A. Transmitted wave

According to the analysis given above, in the region $n \geqslant 0$ there is only a transmitted wave which, following Refs. [34] and [35], can be written as

$$\psi_n = \sum_{m=1}^{\infty} \sum_{l \leqslant m} \mu^m V^{(m,l)}(\eta,\tau) E_n^{(l)}, \tag{2}$$

where $\mu \ll 1$ is the smallness parameter that guarantees that the nonlinear term in Eq. (1) can be treated as a small perturbation to the linear terms. Here, in order to describe the wave envelope, the set of "slow variables," $\tau = \mu^2 n$ and $\eta = \mu(n - v_r t)$, is introduced. By definition, $E_n^{(l)} = \exp(il[k_r n - \omega_r t])$, and ω_r is given by the dispersion relation:

$$\omega_r = -\varepsilon_r - 2C\cos(k_r). \tag{3}$$

In addition, v_r is the group velocity:

$$v_r = \frac{d\omega_r}{dk_r} = 2C\sin(k_r). \tag{4}$$

Inserting Eq. (2) into Eq. (1) gives the NLS equation for a slowly varying envelope $V^{(1,1)}(\eta,\tau)$,

$$iV_\tau^{(1,1)} + \frac{D_r}{2} V_{\eta\eta}^{(1,1)} + N_r |V^{(1,1)}|^2 V^{(1,1)} = 0, \tag{5}$$

with

$$D_r = \cot(k_r) \tag{6}$$

and

$$N_r = \frac{1}{2}\frac{N}{C\sin(k_r)}. \tag{7}$$

The slow variables in the subscripts denote the corresponding partial derivatives, i.e., $f_\tau \equiv \partial f/\partial\tau$, etc.

It should be stressed that Eq. (5) describes the transmitted wave in the reference frame moving with the group velocity v_r.

B. Reflected wave

In the region $n < 0$ there are incident and reflected waves. Note that, in Eq. (1) inhomogeneity is introduced through the linear term only. This implies that, in the reflection process, neither a carrier wave frequency shift nor a scattered pulse Fourier spectrum distortion is present. It should be noted as well that the incident pulse is assumed to be broad enough, and respectively, its spectral width is narrow. Therefore, the incident and reflected waves must have opposite wave numbers, and ψ_n reads [34,35]

$$\psi_n = \sum_{m=1}^{\infty} \sum_{l+l' \leqslant m} \mu^m U^{(m,l,l')}(\xi,\bar{\xi},\tau) E_n^{(l,l')}; \tag{8}$$

here $E_n^{(l,l')} = \exp(il[k_l n - \omega_l t] - il'[k_l n + \omega_l t])$, and the additional slow variables $\xi = \mu(n - v_l t)$ and $\bar{\xi} = \mu(n + v_l t)$ are introduced. In addition,

$$\omega_l = -\varepsilon_l - 2C\cos(k_l) \tag{9}$$

and

$$v_l = \frac{d\omega_l}{dk_l} = 2C\sin(k_l). \tag{10}$$

In general, $U^{(m,l,l')}$ envelopes are allowed to be functions of all (that is, τ, ξ, and $\bar{\xi}$) variables.

Again, inserting Eq. (8) into Eq. (1) gives the NLS equations for slowly varying envelopes. In particular, the perturbation analysis shows that the envelope of an incident wave does not depend on $\bar{\xi}$ [i.e., $U^{(1,1,0)} = U^{(1,1,0)}(\xi,\tau)$] and obeys

$$iU_\tau^{(1,1,0)} + \frac{D_l}{2} U_{\xi\xi}^{(1,1,0)} + N_l |U^{(1,1,0)}|^2 U^{(1,1,0)} = 0. \tag{11}$$

Analogously, the envelope of a reflected wave is independent of ξ [i.e., $U^{(1,0,1)} = U^{(1,0,1)}(\bar{\xi},\tau)$], and

$$iU_\tau^{(1,0,1)} - \frac{D_l}{2} U_{\bar{\xi}\bar{\xi}}^{(1,0,1)} - N_l |U^{(1,0,1)}|^2 U^{(1,0,1)} = 0. \tag{12}$$

In the expressions given by Eqs. (11) and (12), D_l is defined as

$$D_l = \cot(k_l), \tag{13}$$

and the nonlinear coefficient reads

$$N_l = \frac{1}{2}\frac{N}{C\sin(k_l)}. \tag{14}$$

Equations (11) and (12) are written in reference frames moving with the group velocities v_l and $-v_l$, respectively.

C. Boundary conditions

Therefore, the nonlinear wave dynamics on both sides of the discontinuity is governed by the corresponding NLS equations. The boundary conditions at the interface relate the amplitudes of transmitted and reflected waves to that of the incident wave. Indeed, at $n = 0$ Eq. (2) reads

$$\psi_0 = \sum_{m=1}^{\infty} \sum_{l \leqslant m} \mu^m V^{(m,l)} E_0^{(l)}. \tag{15}$$

At the same site Eq. (8) gives approximately

$$\psi_0 \approx \sum_{m=1}^{\infty} \sum_{l+l' \leqslant m} \mu^m U^{(m,l,l')} E_0^{(l,l')}. \tag{16}$$

Note that at $n = 0$ the slow variables are

$$\tau = 0, \quad \eta = -\mu v_r t, \quad \xi = -\bar{\xi} = -\mu v_l t.$$

Analogously, according to Eq. (8), at $n = -1$,

$$\psi_{-1} = \sum_{m=1}^{\infty} \sum_{l+l' \leqslant m} \mu^m U^{(m,l,l')} E_{-1}^{(l,l')}, \tag{17}$$

and Eq. (2) yields the following approximate expression:

$$\psi_{-1} \approx \sum_{m=1}^{\infty} \sum_{l \leqslant m} \mu^m V^{(m,l)} E_{-1}^{(l)}. \tag{18}$$

At $n = -1$ the slow variables read

$$\tau = -\mu^2, \quad \eta = -\mu(1 + v_r t),$$
$$\xi = -\mu(1 + v_l t), \quad \bar{\xi} = -\mu(1 - v_l t).$$

Taking into account that

$$\omega_l = \omega_r \tag{19}$$

must hold in the wave scattering process, Eqs. (15) and (16) give

$$V^{(1,1)} = U^{(1,1,0)} + U^{(1,0,1)}. \tag{20}$$

Moreover, Eqs. (18) and (17) in combination with Eq. (19) result in

$$\exp(-ik_r)V^{(1,1)} = \exp(-ik_l)U^{(1,1,0)} + \exp(ik_l)U^{(1,0,1)}. \tag{21}$$

Here, the Taylor series expansions of $V^{(1,1)}$, $U^{(1,1,0)}$, and $U^{(1,0,1)}$ are employed, and only the corresponding leading terms are kept:

$$V^{(1,1)}(-\mu v_r t - \mu, -\mu^2) \approx V^{(1,1)}(-\mu v_r t, 0),$$
$$U^{(1,1,0)}(-\mu v_l t - \mu, -\mu^2) \approx U^{(1,1,0)}(-\mu v_l t, 0),$$
$$U^{(1,0,1)}(+\mu v_l t - \mu, -\mu^2) \approx U^{(1,0,1)}(+\mu v_l t, 0).$$

That approximation is accurate since $\mu \ll 1$. Moreover, it is clear that slowly varying envelopes can be approximately treated as constant on such small length scales.

Finally, Eqs. (20) and (21) yield

$$U^{(1,0,1)}(\bar{\xi}, 0) = R\, U^{(1,1,0)}(-\bar{\xi}, 0), \tag{22}$$

with the reflection coefficient R,

$$R = \frac{\exp(-ik_r) - \exp(-ik_l)}{\exp(ik_l) - \exp(-ik_r)}, \tag{23}$$

and

$$V^{(1,1)}(\eta, 0) = T\, U^{(1,1,0)}(v_l \eta / v_r, 0), \tag{24}$$

with the transmission coefficient T,

$$T = \frac{2i \sin(k_l)}{\exp(ik_l) - \exp(-ik_r)}. \tag{25}$$

It should be noted that $-\pi \leqslant k_l, k_r \leqslant \pi$ [14]. Nevertheless, in addition, they are related through Eq. (19),

$$\cos(k_r) = \cos(k_l) + \frac{\varepsilon_l - \varepsilon_r}{2C}, \tag{26}$$

and so, generally speaking, not for all allowed values of k_l do corresponding real values of k_r exist. Equations (22), (24), and (26) determine the reflected and transmitted waves from the incident pulse.

III. RESULTS

Let us consider soliton propagation and tunneling processes at the interface of a heterostructure (see Fig. 1). As discussed above, except for the discontinuity, weakly nonlinear pulses can be described by the NLS equation. Solutions of the NLS

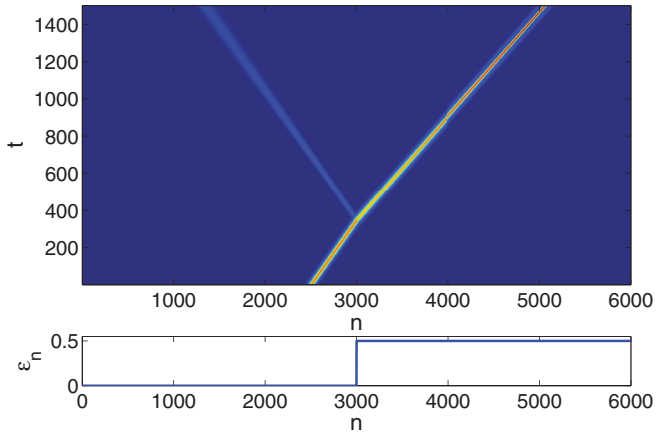

FIG. 1. (Color online) Top: The soliton scattering process at the interface of a heterostructure. Here, $|\psi_n(t)|$ is plotted. Bottom: ε_n as a function of n. In this simulation the interface is located at $n = 3000$. Values of other parameters and further details are given in the text.

model can be studied by means of the inverse scattering method. In particular, the NLS equation

$$i\frac{\partial \Phi}{\partial z} + \frac{P}{2}\frac{\partial^2 \Phi}{\partial x^2} + Q|\Phi|^2\Phi = 0 \tag{27}$$

supports the bright soliton solutions if $PQ > 0$ is satisfied [11,12]. Therefore, in what follows, the values of k_l and k_r are further restricted by $D_l N_l > 0$ and $D_r N_r > 0$ inequalities. In particular, if C and N are simultaneously positive, $|k_l|, |k_r| < \pi/2$, as can be seen from Eqs. (6), (7), (13), and (14). It must be stressed that the analytical method presented is valid for $\pi/2 < |k_l|, |k_r| < \pi$ as well. However, for those values of k_l and k_r, bright soliton solutions do not exist. This case is less interesting for applications and, so, is not considered below.

A. Fundamental soliton scattering

Suppose that the incident pulse represents the fundamental soliton solution of Eq. (11),

$$\Phi(\xi, \tau) = \frac{1}{L}\sqrt{\frac{D_l}{N_l}}\operatorname{sech}\left(\frac{\xi}{L}\right)\exp\left(i\frac{D_l}{2}\frac{\tau}{L^2}\right); \tag{28}$$

here, a real parameter L is the soliton width [12]. Note that L is related to the soliton amplitude as well.

According to Eqs. (22) and (24), the initial conditions for Eqs. (5) and (12), respectively, read

$$\Phi_R(\bar{\xi}, 0) = \frac{R}{L_R}\sqrt{\frac{D_l}{N_l}}\operatorname{sech}\left(\frac{\bar{\xi}}{L_R}\right), \tag{29}$$

$$\Phi_T(\eta, 0) = \frac{v_r}{v_l}\frac{T}{L_T}\sqrt{\frac{D_l}{N_l}}\operatorname{sech}\left(\frac{\eta}{L_T}\right), \tag{30}$$

where $L_R = L$ and $L_T = v_r L / v_l$. In addition, R and T are given by Eq. (23) and Eq. (25). These expressions define the initial value problem for reflected and transmitted waves.

The solution of a sech-type initial value problem of the NLS equation is well known [34–36]. In particular, for the initial

condition,

$$\Phi_i(x,z=0)=\frac{A}{L_i}\sqrt{\frac{P}{Q}}\operatorname{sech}\left(\frac{x}{L_i}\right), \tag{31}$$

the number of generated solitons in Eq. (27) represents the maximum integer M, which obeys

$$M<|A|+\tfrac{1}{2}. \tag{32}$$

In general, $M>1$ and there emerges the bound state of M solitons plus dispersive radiation. The amplitude of the mth soliton is

$$A^{(m)}=\frac{2}{L_i}\sqrt{\frac{P}{Q}}\left(|A|+\frac{1}{2}-m\right). \tag{33}$$

This bound state represents the higher-order soliton solution of the NLS equation with an oscillating profile [11,36]. In the particular case $M=1$, by shedding the dispersive radiation, the solution asymptotically relaxes to a fundamental soliton with a constant shape [see Eq. (28)]. If $|A|\leqslant 1/2$, according to Eq. (32), no soliton can be generated and the pulse disperses. The dispersive modes have vanishing amplitudes in the final state.

Comparison of Eq. (29) with Eq. (31) for a reflected wave directly gives $A=A_R$, where

$$A_R=R, \tag{34}$$

while from Eqs. (30) and (31) for a transmitted wave, it follows that $A=A_T$:

$$A_T=T\sqrt{\frac{D_l}{N_l}}\sqrt{\frac{N_r}{D_r}}\frac{v_r}{v_l}. \tag{35}$$

Equation (26) shows that both A_R and A_T are functions of k_l.

B. Numerical simulations

The incident fundamental soliton scattering process depicted in Fig. 1 represents the solution of Eq. (1) with the initial condition

$$\psi_n(0)=\mu\frac{1}{L}\sqrt{\frac{D_l}{N_l}}\operatorname{sech}(\Xi)\exp(i\Theta), \tag{36}$$

where

$$\Xi=\frac{\mu}{L}(n-n_0), \tag{37}$$

$$\Theta=\left(k_l+\frac{D_l}{2}\frac{\mu^2}{L^2}\right)(n-n_0). \tag{38}$$

Here, it is assumed that the incident fundamental soliton is centered around site $n_0=2500$ at $t=0$. The parameters for numerical calculations are set as follows: $C=N=1$, $L=1$, $\mu=0.05$, $\varepsilon_l=0$, and $\varepsilon_r=0.5$. Equation (26) determines the values of k_r as a function of k_l. Since both C and N are positive, as discussed above, the absolute values of k_l and k_r are chosen to be less than $\pi/2\approx 1.57$. For the given set of parameters the dependency of k_r on k_l is shown in Fig. 2.

The example shown in Fig. 1 corresponds to $k_l=0.8$. The amplitude of the incident soliton [see Eq. (36)] is 0.059. Equations (34) and (35) directly give that $|A_R|=$ 0.188 and $|A_T|=1.37$. Therefore, according to Eq. (32), the reflected pulse represents a dispersive wave packet, and in the transmitted pulse there emerges a fundamental soliton with the amplitude

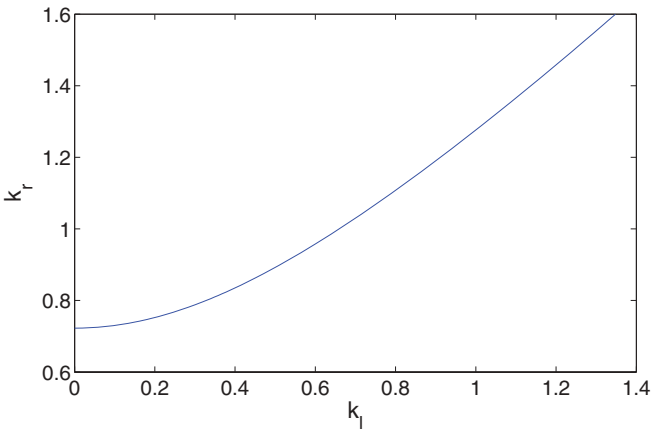

FIG. 2. (Color online) Dependency of k_r on k_l given by Eq. (26). Discussion and the values of other parameters are presented in the text.

$$|\psi_T(t\to\infty)|_{\max}=\mu A_T^{(1)}=0.066, \tag{39}$$

where, following Eqs. (30) and (33), $A_T^{(1)}$ is given by

$$A_T^{(1)}=\frac{2}{L_T}\sqrt{\frac{D_r}{N_r}}\left(|A_T|-\frac{1}{2}\right). \tag{40}$$

During the soliton formation process the pulse amplitude shows a damped oscillatory behavior towards the analytically predicted value. For instance, the arithmetic mean of the maximum and minimum amplitude values in the first oscillation is 0.067. This is in very good agreement with the result predicted by Eq. (39). The amplitude of the reflected pulse, which represents a dispersive wave packet, decays monotonously with time.

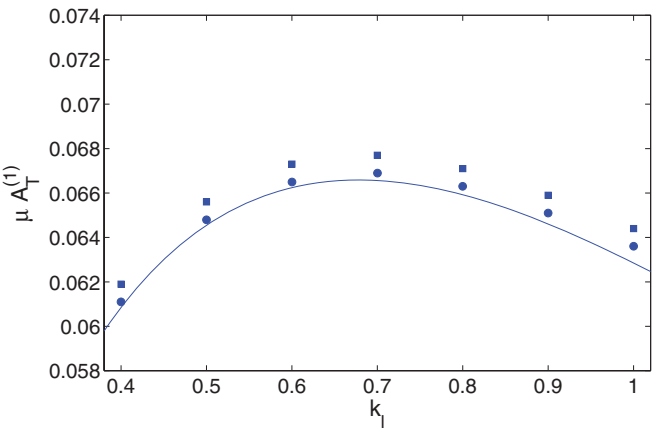

FIG. 3. (Color online) Dependency of $\mu A_T^{(1)}$ on k_l. Squares and circles represent the numerically obtained results for the arithmetic mean of the maximum and minimum amplitude in the first and second oscillations of the soliton parameters, respectively. The solid line is the theoretical prediction.

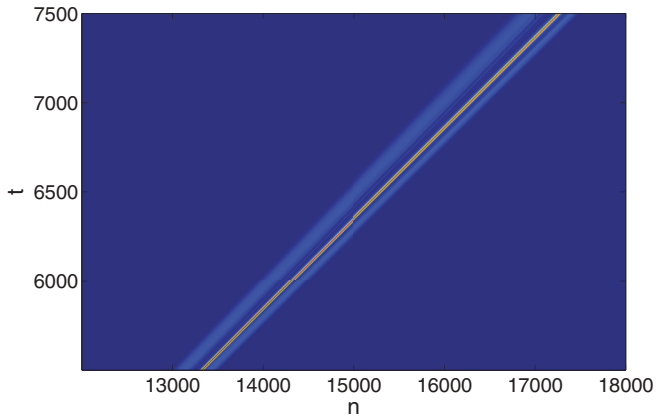

FIG. 4. (Color online) Unstable dynamics of the bound state of two solitons. $k_l = 1.2$, and as in Fig. 1, $|\psi_n(t)|$ is plotted. Higher order effects cause the splitting of the transmitted second-order soliton into two pulses with a long dispersive tail.

According to Eq. (32) a similar dynamics takes place for $0.4 \leqslant |k_l| \leqslant 1.0$. That is, for this range of k_l, a single soliton tunnels at the interface, and the reflected wave represents the dispersive radiation. Figure 3 compares the results of numerical simulations with the analytical predictions. It is difficult to obtain numerically the asymptotic value for the soliton amplitude with arbitrary accuracy. This is the reason for the systematic offset to higher values of the numerical results from the theoretical predictions. Indeed, Fig. 3 demonstrates that the arithmetic mean of the maximum and minimum amplitude values in the second oscillation of the soliton parameters agrees much better with the theory.

For $|k_l| < 0.4$ and $1.0 < |k_l| < \pi/2$ the transmitted pulse is a higher-order soliton. For example, for $k_l = 1.2$ Eqs. (34) and (35) give that $|A_R| = 0.133$ and $|A_T| = 1.838$. That is, the reflected wave represents the dispersive radiation, and the transmitted pulse is the second-order soliton. However, such a bound state is unstable against the neglected higher-order perturbations, and fission of solitons takes place. The process is depicted in Fig. 4. This represents a nonelastic effect which cannot be described by the NLS equation.

Moreover, for the given width of the incident soliton $L = 1$ and $|k_l| < 0.4$, the incident soliton is not sufficiently wide. Indeed, from the definition of ξ and Eq. (28) it follows that the incident wave packet is localized on a scale of order $\sim 2L/\mu \approx 40$. On the other hand, the carrier wavelength is $2\pi/k_l$. For example, for $k_l = 0.3$, this quantity approximately equals . Therefore, the envelope of the pulse cannot be treated as slowly varying. In this case, a larger value for the soliton width, e.g., $L = 2$, must be taken.

IV. DISCUSSION AND CONCLUSIONS

The theory presented reduces the nonintegrable discrete nonlinear Schrödinger equation to the integrable NLS model. This allows us to develop a fully analytical theory of weakly nonlinear solitary wave dynamics in discrete optical heterostructures with a step discontinuity at the interface. It must be stressed that the theoretical results are valid for sufficiently wide solitons.

One of the most interesting processes is lattice soliton tunneling at the interfaces. As demonstrated above, it is possible to derive explicit expressions for the reflected and transmitted pulses from the incident one. The results obtained clearly show that heterostructures represent an effective tool for control and manipulation of soliton amplitude, width, and velocity. The numerical simulations confirm the analytical predictions. Moreover, it is possible to generate higher order solitary pulses from a fundamental soliton. However, unfortunately, such solutions of the NLS equation are unstable against higher-order perturbations, and fission of solitons takes place.

The effects discussed may be useful for the generation and manipulation of slow light pulses, which, in turn, show huge potential for applications in the field of all-optical communications.

ACKNOWLEDGMENTS

I am grateful to R. Khomeriki for useful discussions. This work was supported by the Science and Technology Center in Ukraine (Grant No. 5053).

[1] J. D. Joannopoulos, R. D. Meade, and J. N. Winn, *Photonic Crystals: Molding the Flow of Light*, 2nd ed. (Princeton University Press, Princeton, NJ, 2008).
[2] K. Busch *et al.*, Phys. Rep. **444**, 101 (2007).
[3] M. Campbell, D. N. Sharp, M. T. Harrison, R. G. Denning, and A. J. Turberfield, Nature **404**, 53 (2000).
[4] Y. A. Vlasov, X. Bo, J. C. Sturm, and D. J. Norris, Nature **414**, 289 (2001).
[5] M. R. Jorgensen, J. W. Galusha, and M. H. Bartl, Phys. Rev. Lett. **107**, 143902 (2011).
[6] H. Gersen, T. J. Karle, R. J. P. Engelen, W. Bogaerts, J. P. Korterik, N. F. van Hulst, T. F. Krauss, and L. Kuipers, Phys. Rev. Lett. **94**, 073903 (2005).
[7] Y. A. Vlasov and S. J. McNab, Opt. Lett. **31**, 50 (2006).
[8] M. Notomi, E. Kuramochi, and T. Tanabe, Nature Photon. **2**, 741 (2008).
[9] H. Oda *et al.*, Appl. Phys. Lett. **90**, 231102 (2007).
[10] T. F. Krauss, Nature Photon. **2**, 448 (2008).
[11] G. P. Agrawal, *Nonlinear Fiber Optics*, 3rd ed. (Academic Press, San Diego, 2001).
[12] M. J. Ablowitz, *Nonlinear Dispersive Waves: Asymptotic Analysis and Solitons* (Cambridge University Press, Cambridge, 2011).
[13] Y. S. Kivshar and B. A. Malomed, Rev. Mod. Phys. **61**, 763 (1989).
[14] F. Lederer *et al.*, Phys. Rep. **463**, 1 (2008).
[15] D. N. Christodoulides and R. J. Joseph, Opt. Lett. **13**, 794 (1988).
[16] D. N. Christodoulides and N. K. Efremidis, Opt. Lett. **27**, 568 (2002).

[17] Y. Liu, G. Bartal, D. A. Genov, and X. Zhang, Phys. Rev. Lett. **99**, 153901 (2007).
[18] F. Ye, D. Mihalache, B. Hu, and N. C. Panoiu, Phys. Rev. Lett. **104**, 106802 (2010).
[19] A. Trombettoni and A. Smerzi, Phys. Rev. Lett. **86**, 2353 (2001).
[20] A. Smerzi and A. Trombettoni, Phys. Rev. A **68**, 023613 (2003).
[21] O. Morsch and M. Oberthaler, Rev. Mod. Phys. **78**, 179 (2006).
[22] P. G. Kevrekidis, *The Discrete Nonlinear Schrödinger Equation: Mathematical Analysis, Numerical Computations, and Physical Perspectives* (Springer, Berlin, 2009).
[23] K. G. Makris, S. Suntsov, D. N. Christodoulides, G. I. Stegeman, and A. Hache, Opt. Lett. **30**, 2466 (2005).
[24] S. Suntsov, K. G. Makris, D. N. Christodoulides, G. I. Stegeman, A. Hache, R. Morandotti, H. Yang, G. Salamo, and M. Sorel, Phys. Rev. Lett. **96**, 063901 (2006).
[25] K. G. Makris *et al*., Opt. Lett. **31**, 2774 (2006).
[26] Y. V. Kartashov, L. Torner, and V. A. Vysloukh, Phys. Rev. Lett. **96**, 073901 (2006).
[27] Y. Kominis, A. Papadopoulos, and K. Hizanidis, Opt. Express **15**, 10041 (2007).
[28] S. Suntsov *et al*., Opt. Express **16**, 10480 (2008).
[29] A. Szameit *et al*., New J. Phys. **10**, 103020 (2008).
[30] Y. Kominis and K. Hizanidis, Phys. Rev. Lett. **102**, 133903 (2009).
[31] Y. He, D. Mihalache, and B. Hu, Opt. Lett. **35**, 1716 (2010).
[32] T. Taniuti, Prog. Theor. Phys. Suppl. **55**, 1 (1974).
[33] N. Yajima, Prog. Theor. Phys. **58**, 1114 (1977).
[34] T. Iizuka and M. Wadati, J. Phys. Soc. Jpn. **61**, 3077 (1992).
[35] T. Iizuka, H. Amie, T. Hasegawa, and C. Matsuoka, J. Phys. Soc. Jpn. **65**, 3237 (1996).
[36] J. Satsuma and N. Yajima, Prog. Theor. Phys. Suppl. **55**, 284 (1974).